# Evaluation of possible penstock fatigue resulting from secondary control for the grid

**C. Nicolet**
Power Vision Engineering sàrl
Chemin des Champs-Courbes 1
CH-1024 Ecublens
Switzerland

**R. Berthod**
Stucky SA
Rue du Léman 12
CH – 1920 Martigny
Switzerland

**N. Ruchonnet**
Laboratory for Hydraulic Machines
Avenue de Cour 33 bis
EPFL
CH-1007 Lausanne
Switzerland

**F. Avellan**
Laboratory for Hydraulic Machines
Avenue de Cour 33 bis
EPFL
CH-1007 Lausanne
Switzerland

## Abstract

Due to electricity market deregulation, the contribution of hydroelectric power plants to secondary control becomes of major interest regarding the electrical grid stability. Besides the grid stability improvements obtained with secondary control, the power utilities are more and more concerned by the influence of the constantly changing power set point on the lifetime of the power plant components. The pumped storage power plant of Moiry-Mottec owned by Forces Motrices de la Gougra SA in Switzerland of 69MW, was originally commissioned in 1960. The power plant featuring complex hydraulic layout comprises 3 Pelton units of 23MW, one storage pump of 24MW and one siphon pump of 7.5MW. Since 2009, 2 units of this power plant provide secondary control services to the grid in generating mode. If inspections and related maintenance can be done rather easily for turbines, pumps and generators parts, these tasks are more difficult to undertake for the penstock. This paper addresses the solicitations of the penstock resulting from the new control mode analyzed by means of numerical simulation for predicting possible fatigue of the penstock materials. To carry out this analysis, a simulation model is elaborated using the simulation software SIMSEN and includes the upstream reservoir, the gallery, the surge tank, the penstock, the Pelton turbines and the control loops for secondary control of active power. First, the simulation model is presented and validated with in-situ measurements carried out in case of both prequalification and secondary control. Then, time domain simulations are carried out considering 3 different types of active power set point signals: (i) Pseudo-Random signal, (ii) triangle signals and (iii) real secondary control set point history. Finally, the pressure amplitudes resulting from the simulation are converted into penstock materials stress to carry out fatigue analysis. The fatigue analysis accounts for welding details and enables defining allowable number of cycle along the penstock.

## 1. Introduction

Due to flexible output power, fast output power changes and extended operating range, hydroelectric power plants play a strong role in the stability of electrical power networks. Indeed, hydroelectric power plants can contribute to primary, secondary and tertiary control as well as voltage support ancillary services. To provide such services, hydropower plants must comply with prequalification tests defined by the Transmission System Operator, TSO. In Switzerland, the Transmission System Operator Swissgrid has the following requirements for hydropower plants [11]:

- **for primary control:** power setpoint changes within maximum 30s;
- **for secondary control:** power setpoint change within maximum 5 minutes, minimum control rang of +/-5MW and minimum output power change rate of 0.5% of the rated output power per second;
- **for tertiary control:** power setpoint changes within 15minutes.

The 3x23MW pumped storage power plant of Mottec, located in the canton Valais of Switzerland and owned by "Forces Motrices de la Gougra SA" [1], successfully fulfilled the Swissgrid prequalification tests for primary and secondary control services in year 2008. Since 2009, two Pelton turbine units provide secondary control services and are experiencing constantly changing active power setpoint as presented in Figure 1. As consequence, the position of the needles of the Pelton turbines is also constantly changing in order to follow up the output power setpoint transmitted by Swissgrid and induces pressure fluctuations in the penstock. If, the effect of secondary control on the generation units can be handled by appropriate inspection and maintenance policy, the consequences on the penstock safety is more complex to harness. Therefore, the possible fatigue of the penstock commissioned in 1960 is of particular interest.

This paper presents the investigation carried out to evaluate the possible fatigue of the penstock of Moiry-Mottec power plant by means of numerical simulation. The overall methodology applied for this project is presented in

Figure 2. First, a simulation model of the power plant is setup using the simulation software SIMSEN. This simulation model takes into accounts the hydraulic waterways, the turbines characteristics and the turbine governor. This simulation is validated by comparison of simulation results with on site measurements carried out in case of Secondary Control. Then, time domain simulations are carried out considering three different types of power setpoint: (i) white noise excitation signal in order to compute system transfer function and identify the dynamic characteristics of the power plant, (ii) triangle signals at frequencies of particular interest identified from transfer function in order to calculate peak-to-peak pressure amplitude along the penstock and (iii) real secondary control signal to compare with the results obtained with triangle signals. Finally, the pressure amplitudes obtained along the penstock are converted into material stresses in the penstock to compare with admissible fatigue stresses according to constructive details of the penstock.

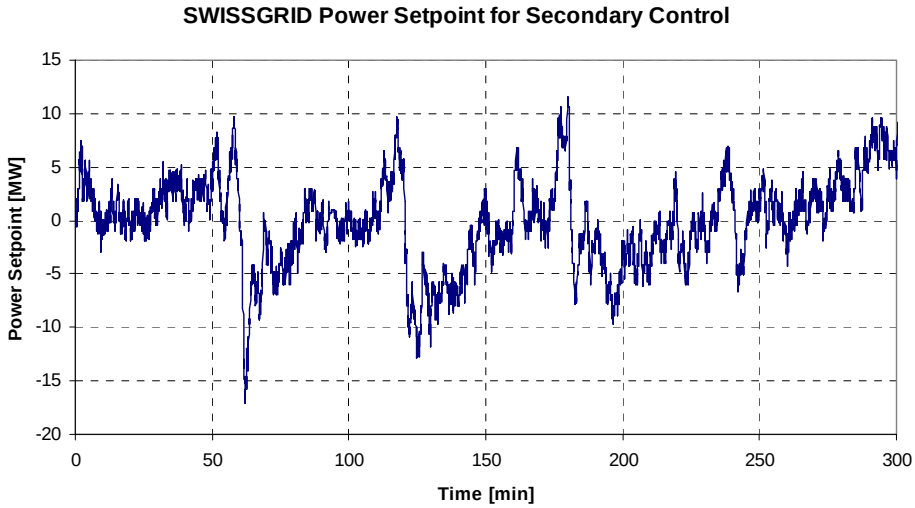


*Figure 1: Typical power setpoint for secondary control of Mottec Power Plant.*

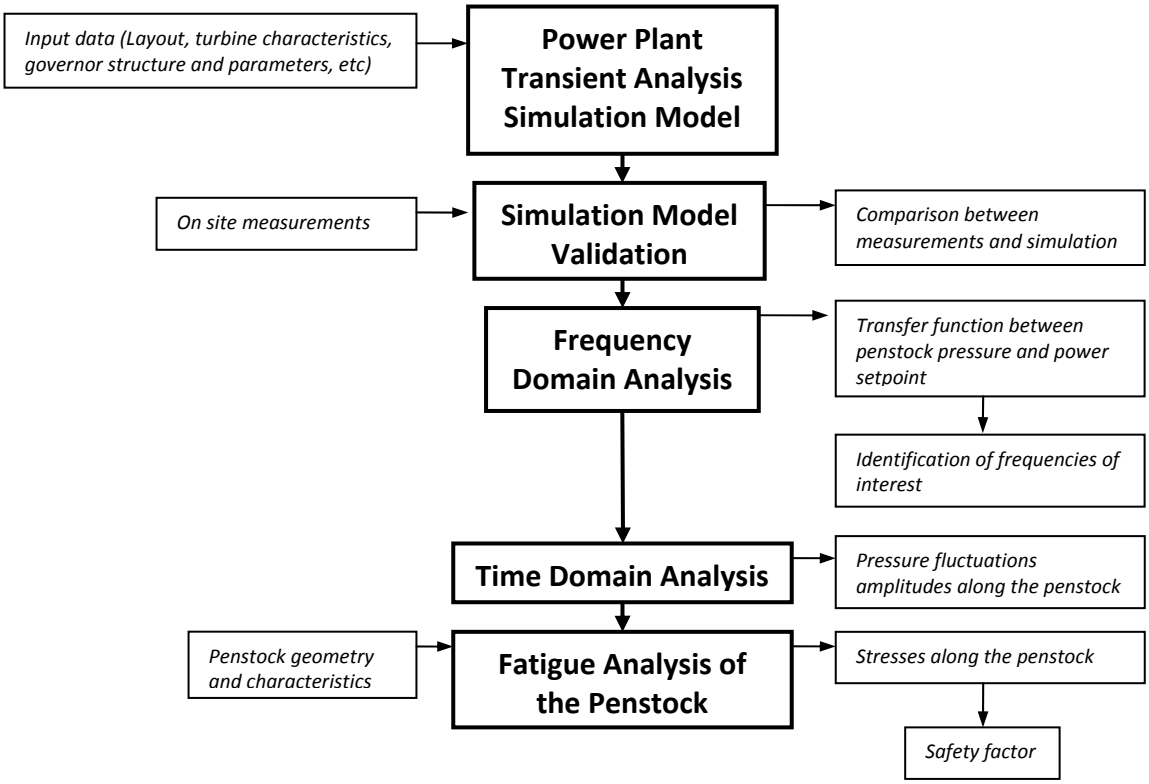


*Figure 2: General approach applied to evaluate the risk of penstock fatigue.*

## 2. Moiry-Mottec Pumped Storage Power Plant

The layout of the Moiry-Mottec pumped storage power plant is presented in Figure 3. The power house of Mottec is connected to two upstream reservoirs: (i) the Moiry reservoir with maximum water level of 2249masl and capacity of 77 millions cubic meters and the Tourtemagne reservoir with maximum water level of 2177masl and capacity of 0.77 millions cubic meters. Each adduction system comprises a gallery, a surge tank and a penstock. This investigation focuses on the adduction between Moiry and Mottec comprising:

- **the upper reservoir of Moiry**: maximum water level Zmax=2249masl, minimum water level Zmin=2150masl;
- **the gallery:** 3380m long with diameter of 2.4m;
- **the surge tank of Tsarmette:** with lower and higher expansion chambers;
- **the penstock of Tsarmette**: total length of 1180m and diameter from 2.1m to 1.5m;
- **the Mottec power house:** with 3 Pelton units of 23MW, a storage pump of 24MW and a siphon pump of 7.5MW;
- **the lower reservoir of Mottec**: maximum water level Zmax=1561masl, minimum water level Zmin=1552masl.

The main characteristics of the 3 units of the Mottec power house shown in Figure 4 are given in Table 1. Figure 5 shows a cut view of the unit 2 comprising one Pelton turbine and the storage pump.

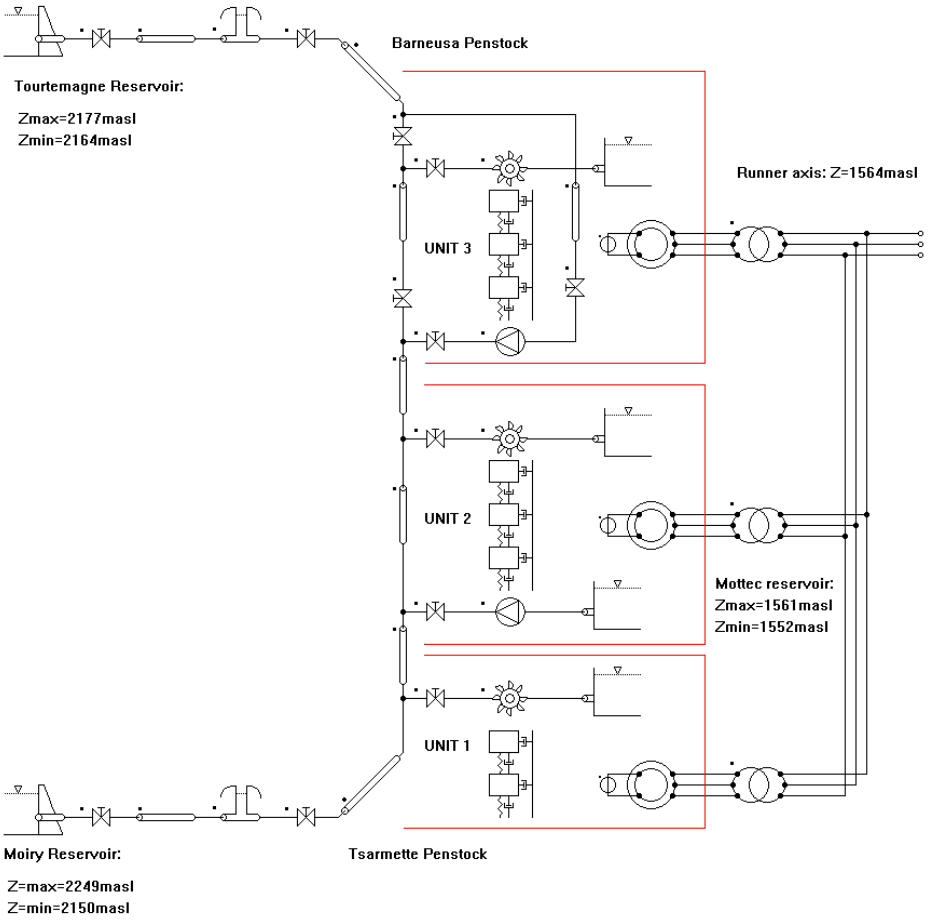


*Figure 3: Moiry-Mottec power plant layout and SIMSEN simulation model.*

**Table 1** Machines characteristics.

| **Pelton turbine** | **Generator** | **Storage Pump** | **Siphon Pump** |
|---|---|---|---|
| $P_R$=23 MW<br>$N_R$=750 rpm<br>$Q_R$=4 $m^3/s$<br>$H_R$=656 mWC<br>2 runners per unit<br>2 injectors per runner | Rated apparent power: 29 MVA<br>Rated phase to phase voltage: 9kV<br>Frequency: 50 Hz | $P_R$=24MW<br>$N_R$=750rpm<br>$Q_R$=3.6m3/s<br>$H_R$=600mWC<br>Nb. Stages: 3 | $P_R$=7.5MW<br>$N_R$=750rpm<br>$Q_R$=5m3/s<br>$H_R$=126mWC<br>Nb. Stages: 1 |

*Figure 4: Pelton units of Mottec power plant.*

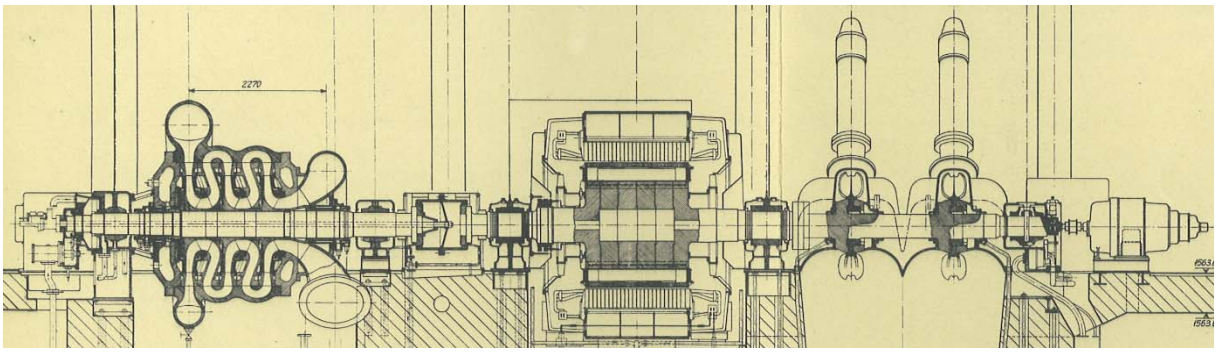


*Figure 5: Cut view of the ternary unit 2.*

## 3. Modeling of the Hydraulic Machinery and Systems

By assuming uniform pressure and velocity distributions in the cross section and neglecting the convective terms, the one-dimensional momentum and continuity balances for an elementary pipe filled with water of length *dx*, cross section *A* and wave speed *a*, see Figure 6, yields to the following set of hyperbolic partial differential equations [13]:

$$\begin{cases} \dfrac{\partial h}{\partial t} + \dfrac{a^2}{gA} \cdot \dfrac{\partial Q}{\partial x} = 0 \\ \dfrac{\partial h}{\partial x} + \dfrac{1}{gA} \cdot \dfrac{\partial Q}{\partial t} + \dfrac{\lambda |Q|}{2gDA^2} \cdot Q = 0 \end{cases} \tag{1}$$

The system (1) is solved using the Finite Difference Method with a 1st order center scheme discretization in space and a scheme of Lax for the discharge variable. This approach leads to a system of ordinary differential equations that can be represented as a T-shaped equivalent scheme [3], [6], [10] as presented in Figure 7. The RLC parameters of this equivalent scheme are given by:

$$R = \frac{\lambda \cdot \left|\overline{Q}\right| \cdot dx}{2 \cdot g \cdot D \cdot A^2} \qquad L = \frac{dx}{g \cdot A} \qquad C = \frac{g \cdot A \cdot dx}{a^2} \tag{2}$$

Where λ is the local loss coefficient. The hydraulic resistance R, the hydraulic inductance L, and the hydraulic capacitance C correspond respectively to energy losses, inertia and storage effects.

The model of a pipe of length $L$ is made of a series of $n_b$ elements based on the equivalent scheme of Figure 7. The system of equations relative to this model is set-up using Kirchoff laws. The model of the pipe, as well as the models of valve, surge tank, hydraulic turbines, etc, are implemented in the EPFL software SIMSEN developed for the simulation of the dynamic behavior of hydroelectric power plants, [4], [7]. The time domain integration of the full system is achieved in SIMSEN by a Runge-Kutta 4$^{th}$ order procedure.

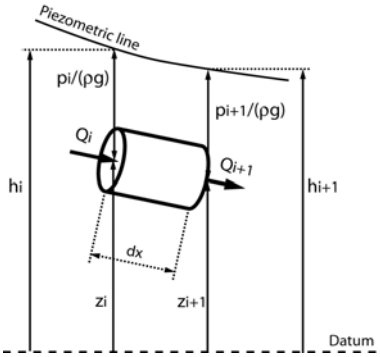


*Figure 6: Elementary hydraulic pipe of length dx.*

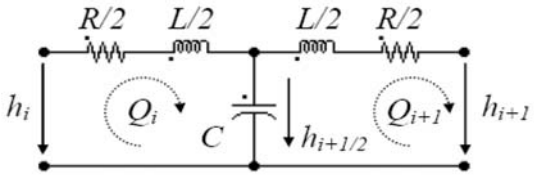


*Figure 7: Equivalent circuit of an elementary pipe of length dx.*

The modeling approach based on equivalent schemes of hydraulic components is extended to all the standard hydraulic components such as valve, surge tanks, air vessels, cavitation development, Francis pump-turbines, Pelton turbines, Kaplan turbines, pump, etc, see [4].

The SIMSEN model of the Moiry-Mottec power plant is presented in Figure 3. This simulation model accounts for waterhammer, mass oscillation, turbine characteristics effects. The model also includes a model of the turbine governor. The electrical components and the pumps are not considered for this investigation and the valves connecting to the reservoir of Tourtemagne at the bottom of the penstock of Barneusa are closed.

## 4. Secondary Control Modeling and Validation

### 4.1. Secondary Control Modeling

The block diagram of the governor of the Pelton turbines of Mottec power plant is presented in Figure 8. This governor comprises a Proportional Integral Derivative (PID) speed governor with permanent speed droop for primary control and a PID power governor enabling secondary control, [2], [12]. For this investigation, it is assumed that the secondary control has a major contribution to the possible fatigue of the Tsarmette penstock as the power setpoint is constantly changing while the primary control does not contribute to the fatigue as the frequency of the European grid is almost constant and large deviations occur very seldom. Thus, the block diagram of Figure 8 can be reduced to the block diagram of Figure 9.

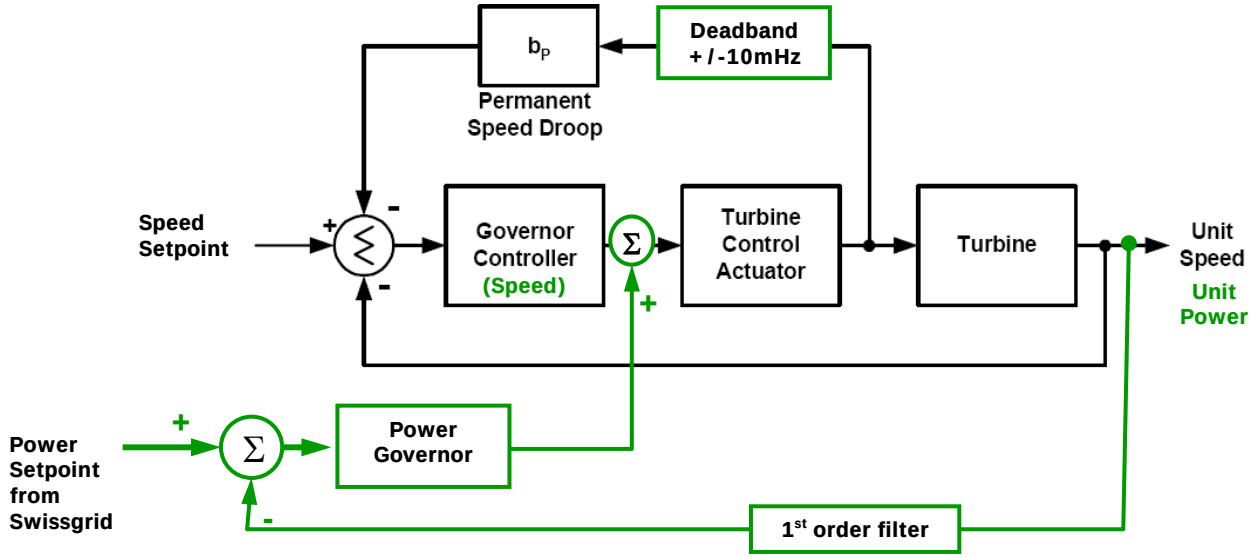


*Figure 8 :Block diagram of control System of Pelton turbines.*

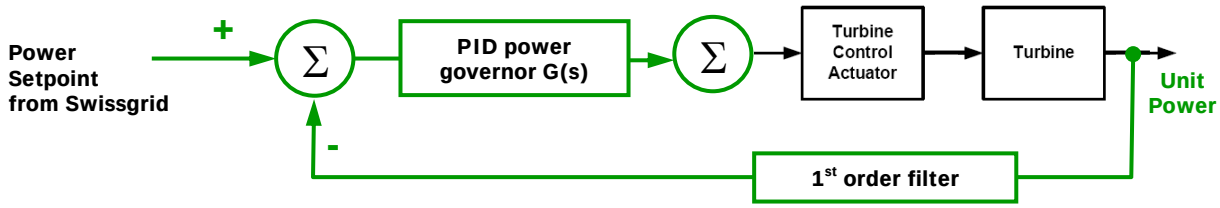


*Figure 9: Simplified model of control System of Pelton turbines.*

The block diagram of secondary control of Figure 9 is included in the SIMSEN model of the power plant and includes:

- a power setpoint defined from Swissgrid;
- the transfer function of PID power governor with series structure;
- the rate limiter for needle positioning;
- a servomotor model with first order time constant and stroke limiter;
- a first order filter on the measured output active power of the unit.

The transfer function of the PID power governor including the 1st order filter is given by:

$$G(s) = K_c \left( \frac{\tau_I \cdot s + 1}{\tau_I \cdot s} \right) \left( \frac{\tau_D \cdot s + 1}{T_{filter} \cdot s + 1} \right) \tag{1}$$

Where :

$$T_I = \tau_I \cdot \alpha \qquad T_D = \frac{\tau_D}{\alpha} \qquad \alpha = 1 + \frac{\tau_D}{\tau_I} \tag{2}$$

With:
$K_c$ : gain [-]
$T_I$ : integral time constant[s]
$T_D$ : derivative time constant [s]
$T_{filter}$ : filter time constant [s]
$s = \sigma + j\omega$ : Laplace operator [1/s]

### 4.2. Model Validation

The simulation of the model of the Moiry-Mottec power plant has been originally validated for standard transient analysis purposes and gave satisfactory simulation results compared to on site measurements. As this model was extended to secondary control, the model of the turbine governor was validated by comparison between simulation results and on site measurements for two cases:

- power setpoint changes for secondary control prequalification tests;
- power setpoint changes during power generation.

The comparisons between simulation results and on site measurements are respectively presented in Figure 10 and Figure 11 and show for both cases good agreements and thus validate the model for secondary control.

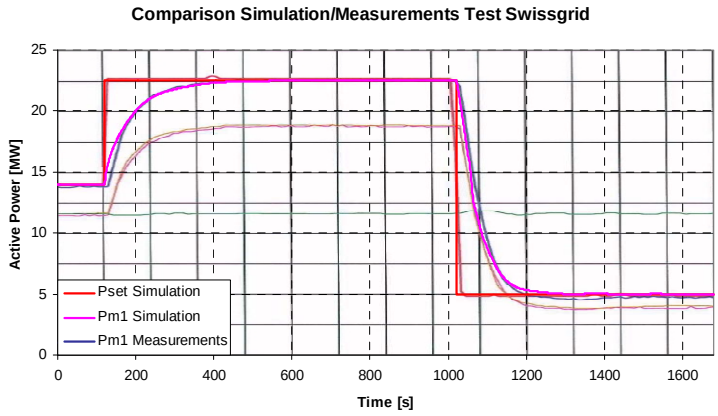


*Figure 10: Comparison between simulation results and on site measurements of power setpoint changes.*

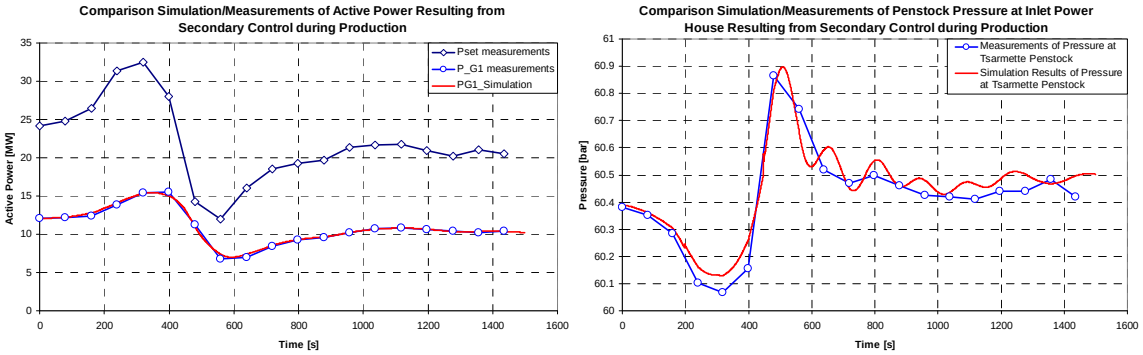


*Figure 11: Comparison between simulation results and on site measurements of secondary control power setpoint changes during generation (left) and pressure at Tsarmette penstock end (right).*

## 5. Determination of Pressure Fluctuations Resulting from Secondary Control

Time domain simulations are carried out considering three different types of power setpoint:

- (i) white noise excitation signal in order to compute system transfer function and identify the dynamic characteristics of the power plant;
- (ii) triangle signals at frequencies of particular interest identified from transfer function in order to calculate peak-to-peak pressure amplitude along the penstock;
- (iii) real secondary control signal to compare with the results obtained with triangle signals.

### 5.1. Frequency Domain Response and System Characterization

Time domain simulation considering white noise excitation as secondary control setpoint is carried out using a pseudo random binary sequence to model the white noise excitation, see [5]. The resulting transfer function between the power setpoint and the pressure at the end of the penstock of Tsarmette is presented in Figure 12. This transfer function points out the natural frequencies of the hydraulic systems.

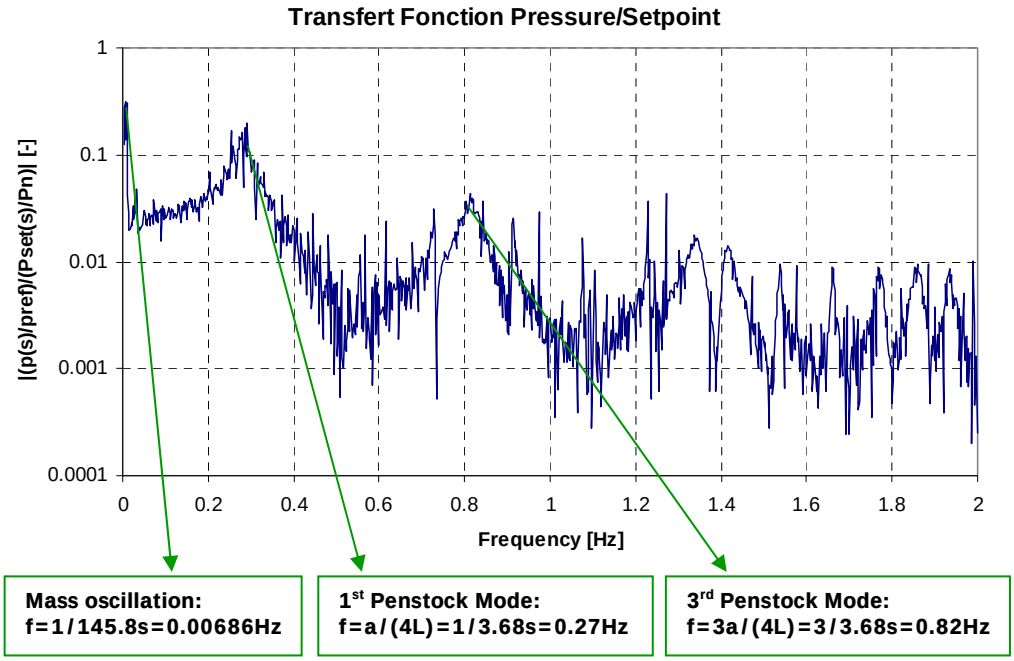


*Figure 12: Amplitude Spectra of the transfer function between pressure fluctuations at penstock end and power setpoint.*

The mass oscillation period between the surge tank and the upper reservoir can be calculated as follows:

$$T_o = 2\pi\sqrt{\frac{l_g \cdot A_{ch}}{g \cdot A_g}} = 2\pi\sqrt{\frac{3380 \cdot (\pi \cdot 3^2/4)}{g \cdot (\pi \cdot 2.4^2/4)}} = 145.8s \quad (3)$$

With : $l_g$ : length of the gallery [m]

$A_{ch}$ : horizontal cross section of the surge tank [m$^2$]

$A_g$ : cross section of the gallery [m$^2$]

The first natural frequency of the penstock corresponding to an open-close pipe can be calculated as follows:

$$f_o = \frac{\bar{a}}{4l} = \frac{1284.7m/s}{4 \cdot 1182m} = 0.272Hz \quad => \quad T_o = \frac{1}{f_o} = 3.68s \quad (4)$$

With : $l$ : total length of the penstock [m]

$\bar{a}$ : average wave speed in the penstock [m/s]

The frequencies of the higher order modes of the penstock for open-close boundary conditions are given by :

$$f_k = (2 \cdot k - 1) \cdot \frac{a}{4l} \quad ; \quad k = 1,2,3,... \quad (5)$$

The values of the system natural frequencies determined analytically correspond well to the values identified from the transfer function of Figure 12. It can be also noticed that the transfer function points also out the anti-resonance frequencies of the penstock obtained for $2k \cdot (a/(4l))$. It can be also noticed that as expected, the higher the order of the mode, the higher damping of the mode.

### 5.2. Time Domain Response and Pressure Amplitudes Determination

In order to determine the pressure fluctuation amplitudes resulting from secondary control, time domain simulations are carried out with a power setpoint featuring triangle signal time evolution, see Figure 13. The minimum/maximum power setpoints are defined according to the turbine secondary control operating range and corresponds to an amplitude of 18MW. The peak-to-peak pressure amplitude resulting from the triangle power setpoint are computed along the penstock for different power setpoint triangle signal periods corresponding to the frequencies identified from the transfer function of Figure 12. Different operating conditions have been considered with different numbers of units in operation, upper reservoir water levels, etc. The peak-to-peak amplitude obtained for two units in secondary control at maximum upper reservoir water level are presented in Figure 14 for the first, second and third penstock natural frequencies and for the mass oscillation period.

It can be noticed that:

- the mass oscillation leads to large pressure fluctuation along the whole penstock, leading to large rated pressure amplitude at the top of the penstock if the low static pressure is considered;
- the first natural mode shape of pressure features maximum pressure amplitudes at the penstock end;
- the third mode amplitudes are lower than the first mode amplitudes on the whole penstock;
- the second mode corresponding to open-open pipe features very low amplitudes on the whole penstock.

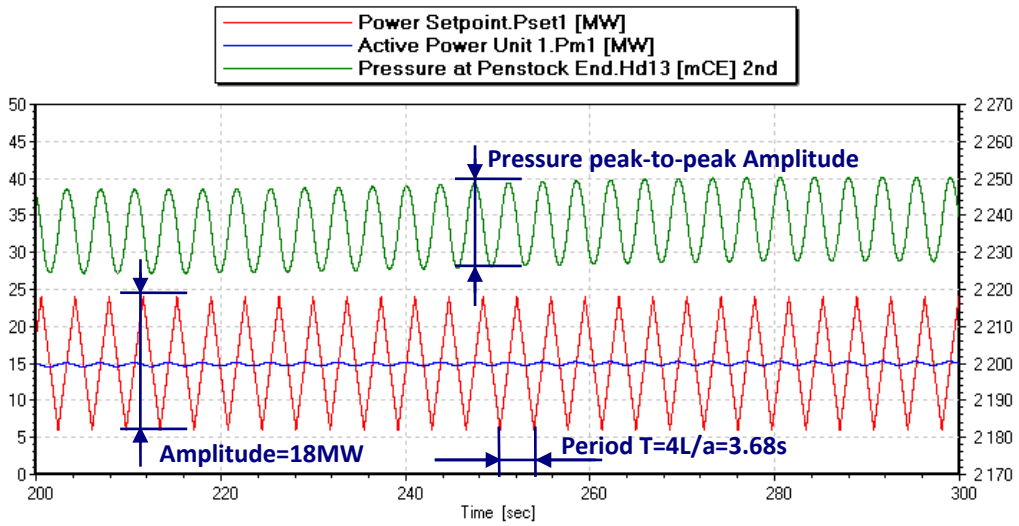


*Figure 13: Time domain simulation with triangle signal setpoint with period corresponding to the first pressure mode shape of the Tsarmette penstock and resulting output active power and pressure fluctuations at the penstock end.*

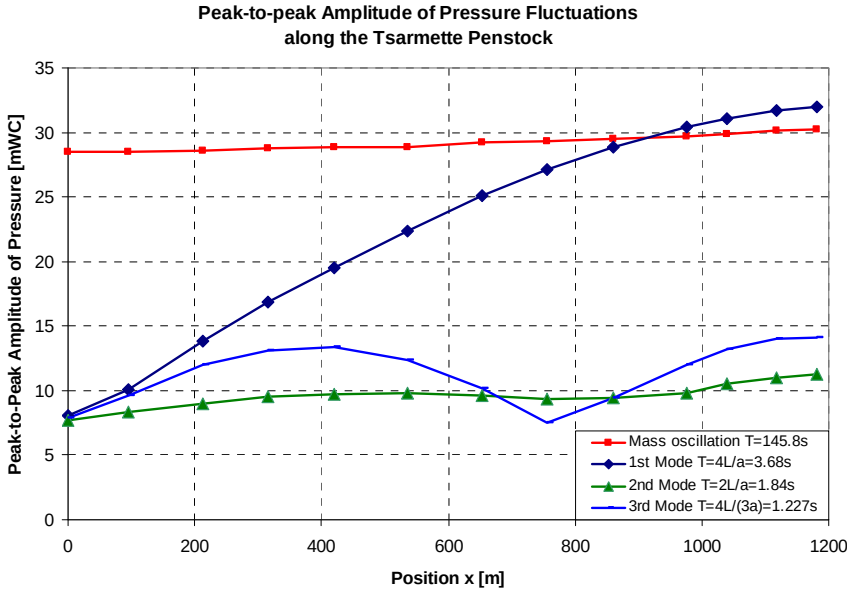


*Figure 14: Peak-to-peak pressure amplitudes along the penstock resulting from time domain simulation with triangle signal setpoint with period corresponding to the first, second and third pressure mode shape of the Tsarmette penstock and to the mass oscillation frequency.*

### 5.3. Time Domain Response to Real Secondary Control Signal

A sample of 4000s of time history is extracted from measurements of secondary control power setpoint of Figure 15 left and is considered in time domain simulation with two different set of PID governor parameters. The existing one and one of a PID governor with time response four time faster, see Figure 16 left. The resulting time domain evolution of the output power of Unit 1 is presented in Figure 16 right for both regulators parameters sets. The resulting peak-to-peak pressure amplitudes along the penstock are presented in Figure 17.

It can be noticed that if the PID governor with faster reaction enables to better follow the power setpoint, it also increases the peak-to-peak amplitudes along the penstock by factor 1.8. It can be also noticed that the shape of the pressure amplitude along the penstock corresponds more or less to the mass oscillation amplitudes shape obtained in Figure 14 but with increasing amplitudes from the top to the end of the penstock. The amplitude spectra of the power setpoint resulting from secondary control of Figure 15 right confirm that this signal contains more energy for the low frequencies in the range of the mass oscillation frequency. However, this result has to be carefully interpreted as the nature of this signal is supposed to be random but it results from the very complex power exchange in the electrical network. Thus, it is subjected to many changes in the coming years as the

electricity market is under constant changes due to increasing role played by renewable energy sources of various types. Therefore, the approach based on the triangular signal seems to be more appropriate even if it is very unlikely that the power setpoint follows such triangular time evolution with frequency corresponding to a natural frequency of the system. Moreover, this approach is very conservative.

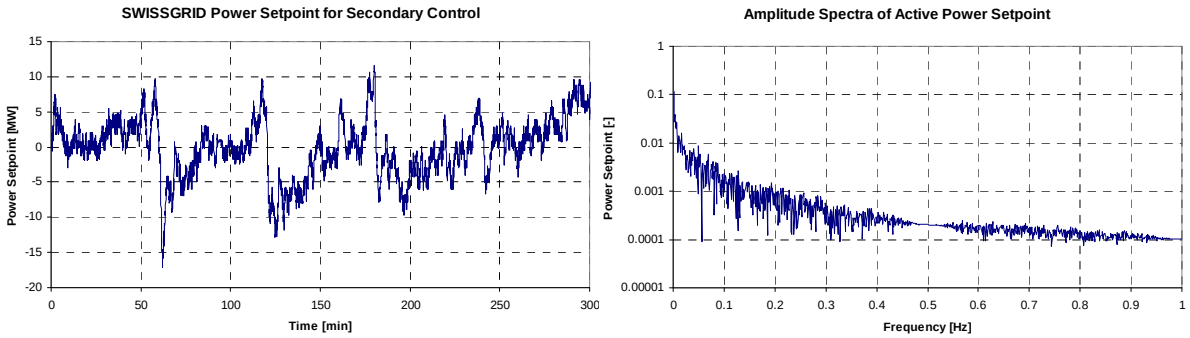


*Figure 15: Typical power setpoint change during secondary control (left) and related amplitude spectra (right).*

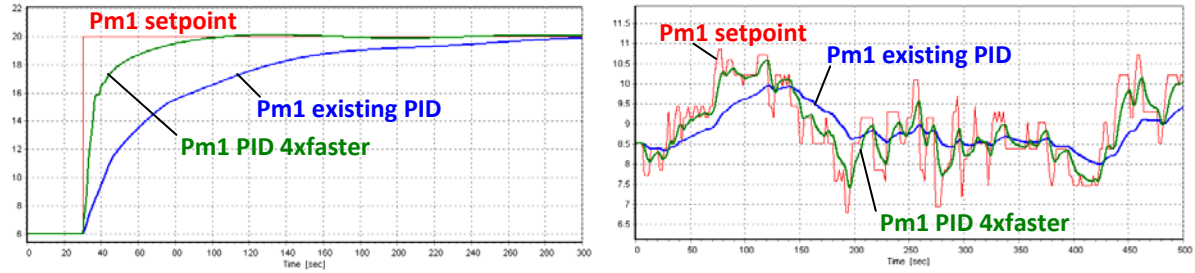


*Figure 16: Comparison of time response of existing PID governor (blue curve) and of a faster PID governor (green curve) (left) and output power of Unit 1 obtained with both governors parameters with a real secondary control signal (right).*

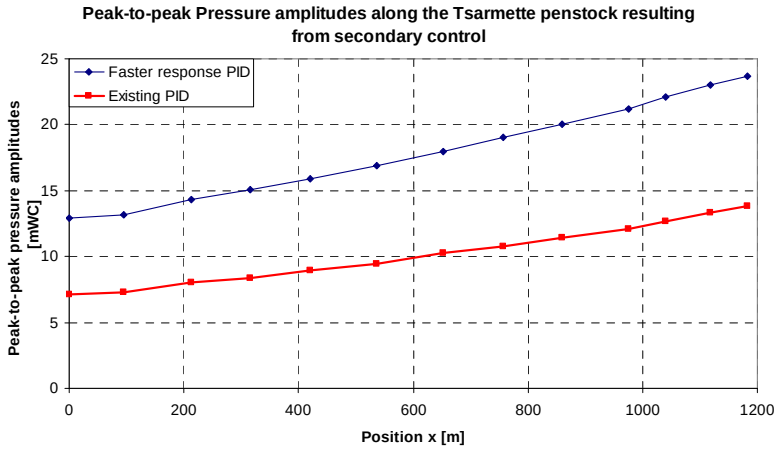


*Figure 17: Peak-to-peak pressure amplitudes along the penstock obtained with the existing PID and a faster PID governor with a real secondary control signal.*

## 6. Fatigue Analysis

The stress amplitude in the pipe walls resulting from pressure fluctuations is computed considering the concrete and rocks surrounding the pipe according to the model of Schleiss [8]. Thus, the stress amplitude in the pipe material is computed as function of the pressure amplitudes $\Delta\sigma = f(\Delta p)$ for each pipe element taking into account the local geology.

The constructive details of the penstock play a major role in the life time prediction of the pipes. The dominant influence of welding details on fatigue resistance is presented as a Wöhler diagram for steel material in Figure 18.

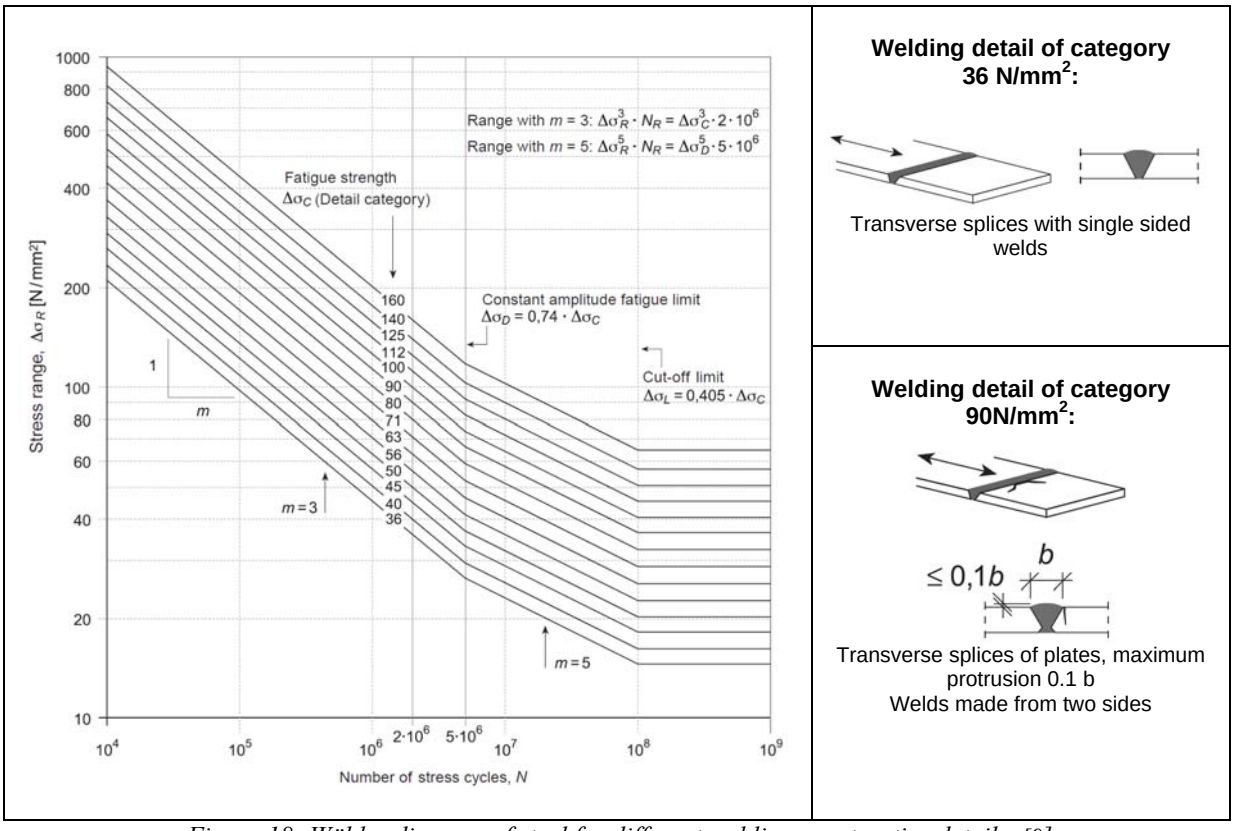


*Figure 18: Wöhler diagram of steel for different welding constructive details, [9].*

The envelopp of pressure amplitudes obtained with triangular signal, see for example Figure 14, are converted into stress variations in the pipe material taking into account the contribution of the pipe surrounding and welding details for different load cases (number of Units in operation, upper reservoir water level, etc.) and represented in the Figure 19 and compared with appropriate Fatigue Limit including safety factor. It can be noticed that for all the cases, the fatigue limit is not reached along the whole penstock ensuring the safety of the penstock with respect to secondary control.

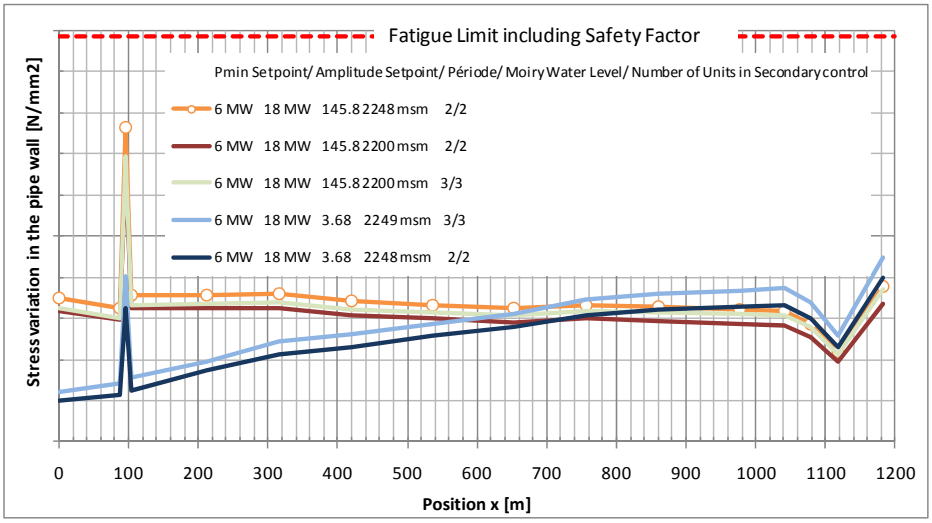


*Figure 19: Pipe material stress along the Tsarmette penstock accounting for welding details of Figure 18.*

## 7. Conclusions

This paper presents the modeling, simulation and analysis of a hydroelectric power plant subjected to secondary control in order to evaluate the possible risk of fatigue of the penstock material. The investigation is carried out by means of time domain numerical simulation with model accounting for waterhammer, mass oscillation, turbine characteristics and turbine governor.

The time domain simulations enabled to point out:

- the dominant effect of the waterways natural frequencies on the pressure amplitude obtained along the penstock;
- that the lower the natural frequency, the higher pressure amplitudes in the penstock;
- the faster time response of the turbine governor, the higher the pressure amplitudes;
- that secondary control signal considered in this investigation features higher energy content for the lowest frequencies, emphasizing the role played by the mass oscillations especially for the upper part of the penstock where the static pressure is usually rather low.

The method using power setpoint defined with triangle signals appears very interesting for the simplicity of signal definition with reduced number of parameters, for the easy interpretation and the conservative aspect of such signal which is very unlikely to occur in real power plant life.

The investigation carried out for the Moiry-Mottec pumped storage power plant showed that the secondary control do not lead to fatigue problem with the existing set of turbine governor parameters. However, it is also important to notice that this investigation does not include possible fatigue effects that may results from normal operation of the power plants inducing several transient phenomena related to turbines/pumps start-up, normal shutdown, emergency shutdown, fast mode change over, etc. These effects would have to be considered in a probabilistic approach involving system solicitations and risk of occurrence.

## 8. Acknowledgements

The authors would like to thank gratefully Mr. Georges-Alain Zuber, Director of Forces Motrices de la Gougra, ALPIQ Suisse SA, and Mr. José Zufferey, Head of Technical Department of Forces Motrices de la Gougra, for their support and contribution of this project and for the authorization to publish these results.

## 9. Nomenclature

A: pipe cross section [$m^2$]
$A_g$: gallery cross section [$m^2$]
$A_{ST}$: surge tank cross section [$m^2$]
$D_{ref}$: machine reference diameter [m]
H: net head [m]
Q: discharge [$m^3/s$]
N: rotational speed [rpm]
P: power [W]
T: Torque [Nm]
a: pipe wave speed [m/s]
h: piezometric head $h=z+p/(\rho g)$ [m]
g: gravity [$m/s^2$]
p: static pressure [Pa]
$l_g$: length of the gallery [m]
p: pressure [Pa]
t: time [s]
x: position [m]
y: turbine guide vane opening [-]
*Z*: elevation above a datum [m]
ν: specific speed $\nu = \omega_R (Q_R / \pi)^{1/2} / (2 \cdot g \cdot H_R)^{3/4}$ [-]
ω: rotational pulsation [rd/s]
R: subscript for rated

### References:


[1] **Forces Motrices de la Gougra**, FMG, website : http://www.gougra.ch.

[2] **IEEE Power Engineering Society,** "IEEE Guide for the Application of Turbine Governing Systems for Hydroelectric Generating Units", IEEE Standards 1207-2004.

[3] **Jaeger, R. C.**, "Fluid transients in hydro-electric engineering practice ".Glasgow: Blackie, 1977.

[4] **Nicolet, C.,** "Hydroacoustic modelling and numerical simulation of unsteady operation of hydroelectric systems", Thesis EPFL n° 3751, 2007, (http://library.epfl.ch/theses/?nr=3751).

[5] **Nicolet, C., Greiveldinger, B., Hérou, J.-J., Kawkabani, B., Allenbach, P., Simond, J.-J., Avellan, F., "**High Order Modeling of Hydraulic Power Plant in Islanded Power Network", IEEE Transactions on Power Systems, Vol. 22, Number 4, November 2007, pp.: 1870-1881.

[6] **Paynter, H. M.,** "Surge and water hammer problems". Transaction of ASCE, vol. 146, p 962-1009, 1953.

[7] **Sapin, A.,** "Logiciel modulaire pour la simulation et l'étude des systèmes d'entraînement et des réseaux électriques", Thesis EPFL n° 1346, 1995, (http://library.epfl.ch/theses/?nr=1346).

[8] **Schleiss, A.,** "Design of reinforced concrete linings of pressure tunnels and schafts", *Hydropower & Dams*, N° 51/52, 88-94, 1997.

[9] **Société Suisse des Ingénieurs et des Architectes,** "Norme 263, Constructions en acier", SIA 2003.

[10] **Souza, O.H., Jr., Barbieri, N., Santos, A.H.M.,** "Study of hydraulic transients in hydropower plants through simulation of nonlinear model of penstock and hydraulic turbine model", IEEE Transactions on Power Systems, vol. 14, issue 4, pp. 1269 – 1272, 1999.

[11] **Swiss Grid-Transmission System Operator**, « Transmission Code 2008 », 2008, (http://www.swissgrid.ch).

[12] **Working group on Prime Mover and Energy Supply Models for System**, "Dynamic Performance Studies. Hydraulic turbine control models for system dynamic studies", Trans. Power Systems 7, 1 (February 1992).

[13] **Wylie, E. B. & Streeter, V.L.,** "Fluid transients in systems". Prentice Hall, Englewood Cliffs, N.J, 1993.


### The Authors


**Christophe Nicolet** graduated from the Ecole Polytechnique Fédérale de Lausanne, EPFL, in Switzerland, and received his Master degree in Mechanical Engineering in 2001. He obtained his PhD in 2007 from the same institution in the Laboratory for Hydraulic Machines. Since, he is managing director and principal consultant of Power Vision Engineering Sàrl in Ecublens, Switzerland. He is also lecturer at EPFL in the field of "Flow Transients in Systems".

**Reynald Berthod** obtained a degree in Civil Engineering from the Ecole Polytechnique Fédérale de Lausanne (EPFL) in 1992. Since then, he is project manager in Stucky S.A. He is in charge of studies concerning hydroelectric power plants and he is expert in dam safety.

**Nicolas Ruchonnet** graduated from EPFL, Ecole polytechnique fédérale de Lausanne, and received a Master degree in Mechanical Engineering in 2004. Since then, he is PhD student at the Laboratory for Hydraulic Machines of the EPFL in field of hydroacoustics

**Prof. François Avellan** graduated in Hydraulic Engineering from INPG, Ecole Nationale Supérieure d'Hydraulique, Grenoble France, in 1977 and, in 1980, got his doctoral degree in engineering from University of Aix-Marseille II, France. Research associate at EPFL in 1980, he is director of the Laboratory for Hydraulic Machines since 1994 and was appointed Ordinary Professor in 2003. Prof. F. Avellan is the Chairman of the IAHR Section on Hydraulic Machinery and Systems.